Molecular Crystals and Liquid Crystals

ISSN: 1542-1406 (Print) 1563-5287 (Online) Journal homepage: http://www.tandfonline.com/loi/gmcl20

Liquid Crystal Channel Waveguides: A Monte Carlo Investigation of the Ordering

A. d'Alessandro, R. Asquini, C. Chiccoli, L. Martini, P. Pasini & C. Zannoni

To cite this article: A. d'Alessandro, R. Asquini, C. Chiccoli, L. Martini, P. Pasini & C. Zannoni (2015) Liquid Crystal Channel Waveguides: A Monte Carlo Investigation of the Ordering, Molecular Crystals and Liquid Crystals, 619:1, 42-48, DOI: 10.1080/15421406.2015.1091156

To link to this article: http://dx.doi.org/10.1080/15421406.2015.1091156

Published online: 23 Oct 2015.

Mol. Cryst. Liq. Cryst., Vol. 619: pp. 42–48, 2015

ISSN: 1542-1406 print/1563-5287 online
DOI: 10.1080/15421406.2015.1091156

Liquid Crystal Channel Waveguides: A Monte Carlo Investigation of the Ordering

A. D'ALESSANDRO,[1] R. ASQUINI,[1] C. CHICCOLI,[2]
L. MARTINI,[1] P. PASINI,[2,*] AND C. ZANNONI[3]

[1]Dept. of Information Engineering, Electronics and Telecommunications, Sapienza University of Rome, Rome, Italy
[2]Istituto Nazionale di Fisica Nucleare, Sezione di Bologna, Bologna, Italy
[3]Dipartimento di Chimica Industriale "Toso Montanari", Università di Bologna and INSTM, Bologna, Italy

We present detailed Monte Carlo (MC) simulations of a nematic cell with homeotropic boundary conditions at the four confining surfaces. The simulations are based on the Lebwohl-Lasher lattice spin model with boundary conditions chosen to mimic the cell anchoring. We have investigated the model using a standard Metropolis Monte Carlo method to study the optical transmission and the ordering through the cell.

Keywords Monte Carlo; confined nematic liquid crystals; anchoring.

Introduction

Confined nematics show peculiar physical phenomena connected to fundamental liquid crystal (LC) properties and to several important applications [1,2]. Recently they have been proposed as effective materials to fabricate both electrically and optically controlled cores for switchable and reconfigurable waveguides [3-6]. In particular optofluidic channels have been successfully proposed by infiltrating LC in polydimethylsiloxane (PDMS) to demonstrate the variation in the diffraction pattern of an array of microfluidic channels acting as a grating [7]. Moreover PDMS is commonly used to create channels for microfluidic applications and recently it was confirmed as an interesting material for optical interconnections to replace metallic wired links, the latter suffering for heat dissipation as well as presenting limitation in high bit rate interconnections [8].

Some of us have recently investigated light propagation in channel waveguides with a core consisting of LC filled PDMS channels (LC:PDMS waveguides). It was shown that polarization independent light transmission takes place despite the typical LC optical anisotropy which in general induces polarization dependence of light propagation [9,10]. A set of rectangular PDMS waveguides of 8, 10 and 15 μm width and 5 μm height has been fabricated (see Fig. 1). The nematic LC (E7) was found to be homeotropically aligned with respect to the PDMS walls, possibly because of the low energy surface of the PDMS

*Address correspondence to P. Pasini, Istituto Nazionale di Fisica Nucleare, Sezione di Bologna, Via Irnerio 46, 40126 Bologna, Italy. E-mail: pasini@bo.infn.it

Color versions of one or more of the figures in the article can be found online at www.tandfonline.com/gmcl.

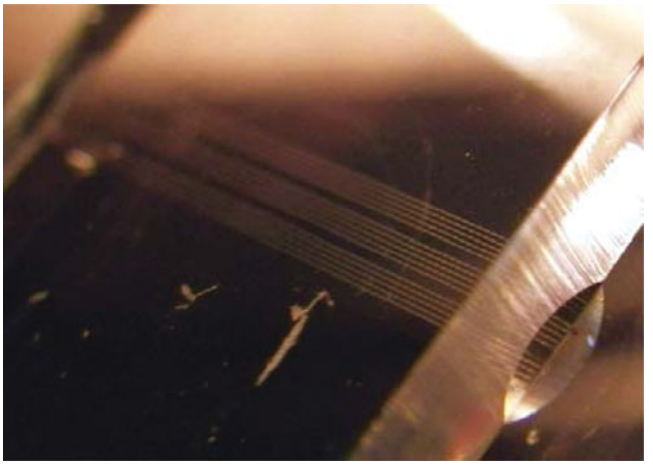

Figure 1. A fabricated prototype with sets of E7 nematic LC straight waveguides.

which results in a minimal contact interface between the rod-like NLC molecules and the PDMS surface. This orientation of LC molecules induced by the interface interaction, at the confining surface walls provides a polarization independent light propagation.

To get a better understanding of this system we wish to present here a detailed investigation of the LC filled cell by means of Monte Carlo simulations. This will allow to reproduce not only polarized optical images but also the molecular organization and the ordering inside the LC system [11].

The Simulation Model

The Monte Carlo simulations were based on the simple and well studied Lebwohl-Lasher (LL) lattice spin model [12,13], the prototype potential for the mesoscale simulations of nematics. The particles interact through the attractive nearest neighbors LL pair potential:

$$U_{i,j} = -\varepsilon_{ij} P_2(\boldsymbol{u}_i \cdot \boldsymbol{u}_j), \tag{1}$$

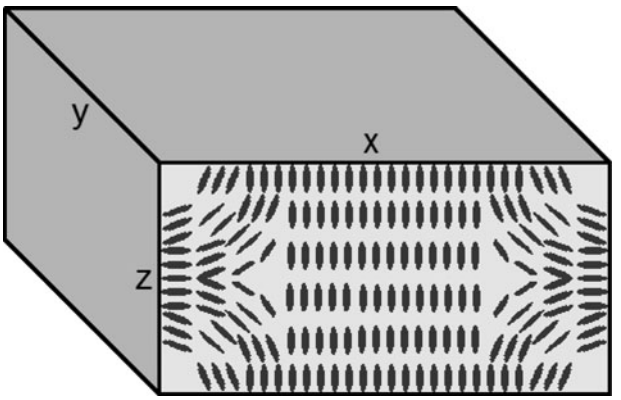

Figure 2. A schematic representation of the cross section of the LC waveguide channel. The boundary conditions are homeotropic at the zy and xy surfaces.

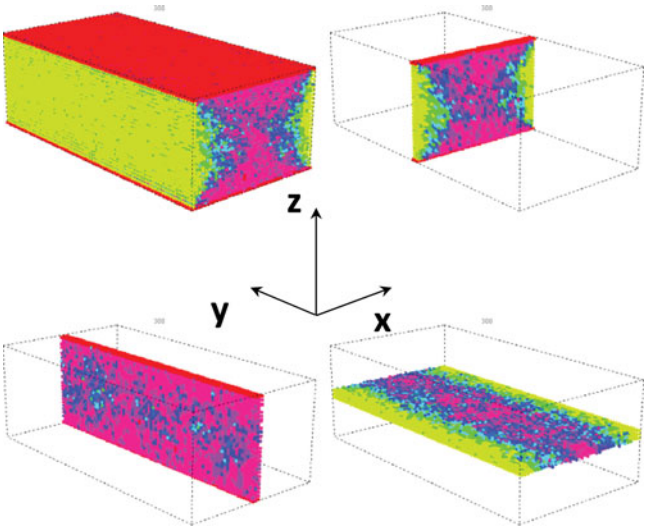

Figure 3. Snapshots of the 40×80×26 system (xyz). The color code indicates the spin orientations with the red one denoting the alignment along z. The first plate (top left) shows the overall molecular organization whereas the other three plates are cross sections taken at the middle layer of each plane (xz, xy, yz) respectively (clockwise).

where:

$$\varepsilon_{ij} = \begin{cases} \varepsilon, & \varepsilon > 0 \quad for\ i, j\ nearest\ neighbours \\ 0 & otherwise, \end{cases} \tag{2}$$

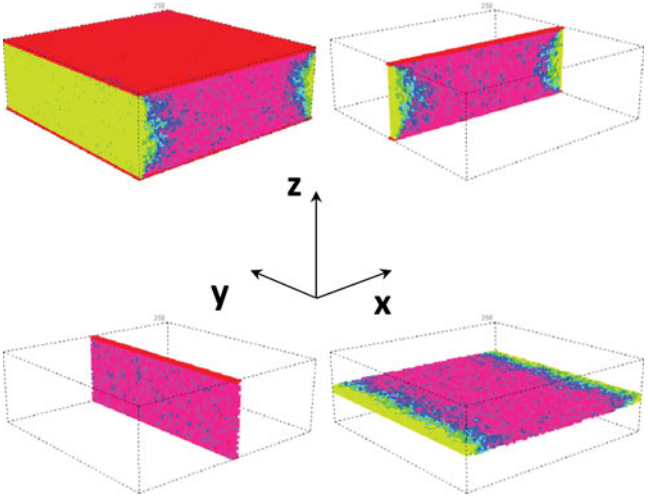

Figure 4. Snapshots of the 80×80×26 system. The color code indicates the spin orientations with the red one denoting the alignment along z. The first plate (top left) shows the overall molecular organization whereas the other three plates are cross sections taken at the middle layer of each plane (xz, xy, yz) respectively (clockwise).

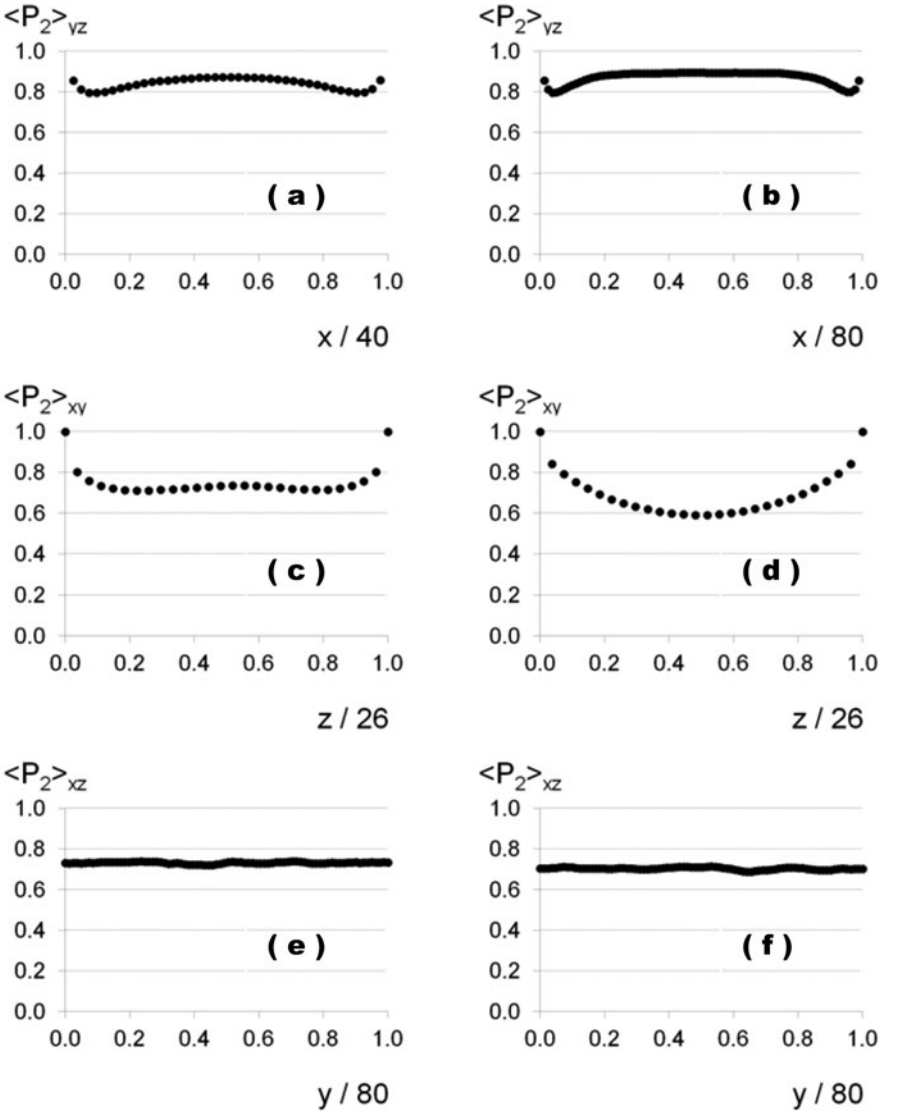

Figure 5. Order parameters calculated at each cross section for the three axes regarding the two system size presented: i.e. 40×80×26 (a, c, e) and 80×80×26 (b, d, f). From top to bottom we show $<P_2>_{yz}$, $<P_2>_{xy}$, $<P_2>_{xz}$ versus the lattice spacings normalized at the maximum values for each system size dimension.

$\boldsymbol{u}_i$, $\boldsymbol{u}_j$ are unit vectors along the axis of the two particles ("spins") and P_2 is a second rank Legendre polynomial. The spins represent a cluster of neighboring molecules whose short range order is assumed to be maintained through the temperature range examined [11]. The bulk Nematic-Isotropic (*NI*) transition occurs for this model at a reduced temperature $T^* \equiv kT / \varepsilon = 1.1232$ [13].

The different boundary conditions of a microchannel are mimicked assuming a layer of outside particles with a fixed orientation consistent with the desired type of alignment at

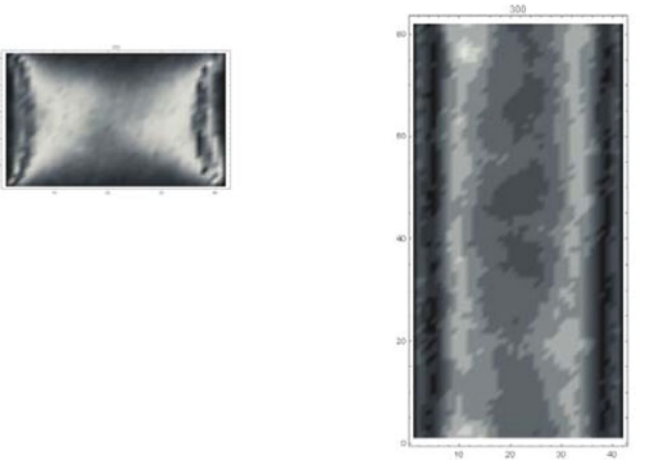

Figure 6. Simulated cross polar optical images obtained from Monte Carlo simulations of a system $40\times80\times26$. A front view is presented on the left, while the right plate shows a vertical point of view.

the surfaces [11]. As we have mentioned before, in this work we need to consider boundary conditions which are homeotropic at four surfaces (see Fig. 2) while for the other two (along the channel) periodic boundary conditions are considered.

The anchoring strength at the surfaces can be tuned by considering a different value of ε_{ij} when the spin j belongs to the additional boundary layers.

To generate the lattice configurations we have used the standard Metropolis Monte Carlo procedure [14] where one spin at a time is updated as described in [11]. Equilibrium Monte Carlo generated configurations have then been used to simulate images corresponding to those observed with polarized light microscopy, an experimental technique used to investigate micrometer size films, starting from the simulated lattice configurations by means of a well tested matrix approach [15,16]. We describe each site in the nematic film as

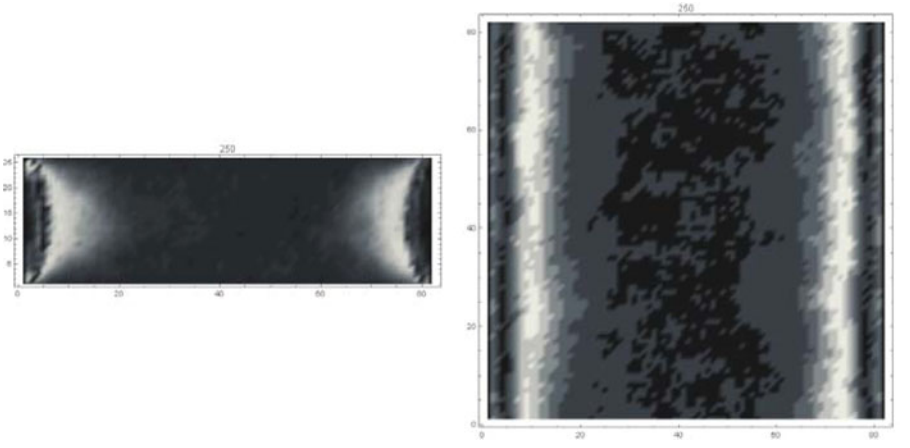

Figure 7. Simulated optical images obtained from Monte Carlo simulations of a $80\times80\times26$ system. A front view is presented on the left, while the right plate shows a vertical point of view.

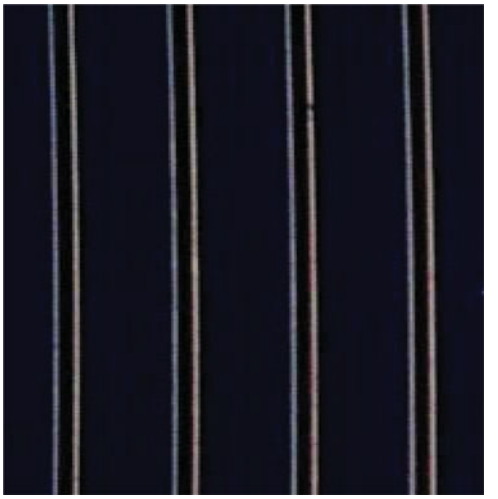

Figure 8. A polarizing microscope image of LC homeotropic alignment in PDMS channels obtained for a produced prototype with sets of E7 nematic LC straight waveguides.

an optical retarder represented by a Müller matrix, so that the light beam travelling through a succession of sites across the layers of the system is retarded by the matrix resulting from the product of the Müller matrices corresponding to each site. The light emerging from each direction of the simulation sample is observed, when required, with the help of crossed polarizers (45 and 135 degrees), placed on two opposite sides of the system, which are represented by appropriate projection matrices and switch off the non retarded light. Finally the light intensity emerging from the system is coded in a scale from black (no light) to white (full intensity) with 32 different grey levels.

Simulation Results

We have performed a set of independent complete simulations for some sizes of the cell mimicking a microchannel of a straight waveguide. Here we report results for a $40\times80\times26$ *(xyz)* and an $80\times80\times26$ lattice where the cross sections of the microchannel are rectangular. Since a spin can represent a cluster of neighboring molecules, we can consider the adopted lattice dimensions compatible with those of the produced waveguides.

In Figs. 3 and 4 we show some typical snapshots of the two systems presented here. It is apparent how the homeotropic surface alignments propagate inside the system. In fact, due the geometry of the system with the horizontal surfaces larger with respect to the other vertical dimensions of the simulated channels, i.e. $z_{max} = 26$ and $x_{max} = 40$, 80 the alignment along z is favored inside the sample.

To give a more quantitative analysis of the ordering inside the systems we have calculated how the order parameter $<P_2>$ varies across each direction of the channel, say at each layer at x,y and z fixed. The results are summarized in Fig 5. Simulations show how the ordering inside the system is affected by the aligning surfaces (see Figs. 5 a, b, c, d) whereas this ordering is constant along the channel (see Fig. 5e and 5f).

As mentioned before we have also simulated the polarizing microscope images starting from the Monte Carlo configurations.

The results, presented in Figs. 6 and 7, show the main features of the experimental observations (see, for example, Fig. 8) even if the simulations concern a single microchannel. We can observe that the intensity of the light is greater for the system with the smaller x dimension. This result should be compatible with the small reduction of the transmitted power as observed in the experiments [10]. In fact the measurements show that, for a given polarization angle, the transmitted power in 9 mm length waveguides is lower in a 15 μm wide waveguide than in a channel of 8 μm width [10].

The present approach can be useful for more detailed investigation to confirm or predict the molecular organization and the ordering induced by particular surface alignments or peculiar geometry of the channels.

Conclusions

We have performed Monte Carlo simulations of a microchannel with a rectangular section, and homeotropic boundary conditions at each wall, filled with a nematic liquid crystal. Our simulations are based on the simplest successful lattice potential put forward to describe nematic liquid crystals (Lebwohl-Lasher). We have employed a standard Metropolis MC method to update the lattice and generate configurations of the confined nematic that we have used to simulate the optics for different geometries and two different sections. The molecular organization of the structure obtained is in good agreement with experimental results and in particular the optical polarized images between crossed polarizers reproduce the experimental observations.

References

[1] Crawford, G. P. and Zumer, S., eds., (1996) *Liquid Crystals in Complex Geometries*, Taylor & Francis, London *and references therein*.
[2] Rasing, T. and Musevic, I.,eds., (2004) *Surfaces and Interfaces of Liquid Crystals*, Springer Verlag, Berlin.
[3] Asquini, R., Fratalocchi, A., d'Alessandro, A., and Assanto, G. (2005). *Applied Optics*, *44*, 4136.
[4] Beeckman, J., Neyts, K., and Vanbrabant, P. J. M. (2011). *Opt. Eng.*, *50*, 081202
[5] Asquini, R., and d'Alessandro, A. (2013). *Liquid Crystals XVII, Proc. SPIE*, *8828*, 88280T
[6] Asquini, R. and d'Alessandro, A. (2013). *Mol. Cryst. Liq. Cryst.*, *572*, 13.
[7] Vasdekis, A. E., Cuennet, J. G., Psaltis, D. (2012). *Liquid Crystals XVI, Proc. of SPIE*, *8475*, 847507.
[8] Missinne, J., Kalathimekkad, S., Van Hoe, B., Bosman, E., Vanfleteren, J., and Van Steenberge, G. (2014). *Optics Express*, *22*, 4168.
[9] Asquini, R., Martini, L., Gilardi, G., Beccherelli, R., and d'Alessandro, A. (2014). *IEEE Photonics Conference (IPC),* San Diego, CA, USA, 12-16 Oct. 2014, Article number 6995197, p. 36.
[10] Asquini, R., Martini, L. and d'Alessandro, A. (2015). *Mol. Cryst. Liq. Cryst.*, *614*, 11.
[11] see for example: Pasini, P., Chiccoli, C. and Zannoni, C. (2000). In *Advances in the Computer Simulations of Liquid Crystals*, P. Pasini and C. Zannoni (eds.), Kluwer, Dordrecht, p. 121.
[12] Lebwohl, P.A. and Lasher, G. (1972). *Phys. Rev. A*, *6*, 426.
[13] a) Fabbri, U. and Zannoni, C. (1986). *Molec. Phys.*, *58*, 763; b) Zhang, Z., Zuckermann, M. J. and Mouritsen, O. G. (1991). *Phys. Rev. Lett.*, *69*, 2803.
[14] Metropolis, N., Rosenbluth, A. W., Rosenbluth, M. N., Teller, A. H. and Teller, E. (1953). *J. Chem. Phys.*, *21*, 1087.
[15] Killian, A. (1993). *Liq. Cryst.*, *14*, 1189.
[16] Ondris-Crawford, R. *et al.* (1991). *J. Appl. Phys.*, *69*, 6380.